Geocenter Motion from a Combination of GRACE Mascon and SLR Data

Claudio Abbondanza[1], Toshio M Chin[1], Richard S Gross[1], Michael B Heflin[1], Jay W Parker[1], Benedikt S Soja[1], David N Wiese[1], Xiaoping Wu[1]

May 6, 2020

[1] Jet Propulsion Laboratory - California Institute of Technology

Jet Propulsion Laboratory
California Institute of Technology

Outline

- Surficial mass variability observed through space gravimetry can be converted into load-induced deformations at Space-geodetic (SG) observing sites by adopting a spectral formalism [9].
- GRACE-derived elastic displacements would represent, if accurate, band-limited load-induced deformations that can be removed from SG-derived station displacements in order to recover degree-1 surface deformation signature, and therefore geocenter motion [3].
- In so doing, the residual SG station displacements, insofar as expressed in a geocentric frame, would reflect a "pure" degree-1 deformation signature that can be recovered via **spectral inversion**.
- We will recover such degree-1 deformation from residual displacements (SG-GRACE) and will compare it to standard geocenter motion solution determined via **network shift** approach.

1. Data Sets

- We adopt GRACE JPL Mascons (RL06) [12] solution available at `https://grace.jpl.nasa.gov/data`
- in conjunction with load Love numbers inferred from **Preliminary Earth Reference Model** [see e.g. 11] to derive load-induced elastic displacements. The assumption we are making here is that (i) Earth's response to loading and mass transport is purely elastic and (i) Earth is isotropic (no lateral variation of its mechanical properties).
- State-of-art SLR solution (weekly station positions and daily EOPs in SINEX format) produced by the Italian Space Agency (ASI) in preparation for the ITRF2020.

2(a). SLR-ASI Data Set

- ASI Preliminary Solution compliant with the ITRF2020 Call for Participation standards.
- In order to improve SLR scale and geocenter, ILRS implements new treatment of station-dependent range biases, mean pole and time variable gravity.
- To match GRACE time span, we restrict ASI-SLR data to the interval 2002-2016, during which 49 stations, not all simultaneously co-observing, are available.
- SLR SINEX files are monthly binned and interpolated at the midpoint epoch of JPL-RL06M GRACE Mascons solutions.

2(b). SLR-ASI vs ILRS2014 - WRMS

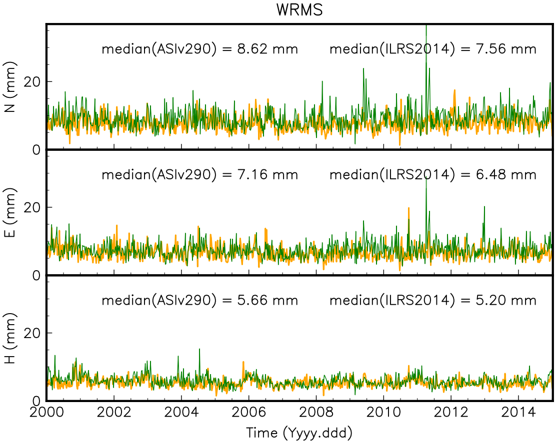

Per-Session Weighted RMS of the Residuals computed after removal of a 7-parameter transformations. Green Curve relates to ASIv290. Orange is ILRS2014.

3. JPL Mascon RL06 (JPL-RL06M) Data Set

- State-of-art JPL Mascon solution (RL06M.MSCNv01) obtained by reducing Level-1 GRACE observations [12] and available on `http://grace.jpl.nasa.gov`
- JPL-RL06M are gridded data types reporting surface mass changes in Equivalent Water Thickness with a spatial sampling of 0.5° in both latitude and longitude.
- **Why Mascons instead of Spherical Harmonic Solutions**?
  - The JPL-RL06M Kalman filter formulation allows direct use of its gravity field products without signal attenuation from smoothing and de-striping.

4. Spectral Properties of JPL-RL06M vs CSR-RL06

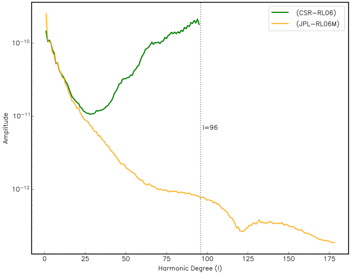

Median amplitude (square root of Equation 1) spectra for JPL-RL06M and CSR-RL06. In both solutions, de-aliasing products were restored and linear trends removed from the Stokes coefficients.
CSR solution is unfiltered, i.e. neither smoothing nor destriping was applied.
JPL solution is spatially and temporally constrained.

- Power Spectrum as a function of the Harmonic Degree:

$$P_\ell = \sum_{m=-\ell}^{+\ell} |c_{lm}|^2 \tag{1}$$

- CSR-RL06 solution is bandlimited up to $\ell = 96$
- JPL-RL06M has been expanded in SH up to $\ell = 179$
- The geophysical signal is approximately concentrated within the spectral band $2 \leq \ell \leq 70$.
- The higher degrees in JPL-RL06M are used to reconstruct the "geometry" of the mascon caps.
- The unfiltered CSR-RL06 solution is dominated by high wavenumber noise ($\ell > 40$), hence the necessity of smoothing/destriping on conventional SH solutions.

5. Elastic Displacements $u(\mathbf{x})$ from JPL-RL06M (a)

- If the surficial load admits a representation in real spherical harmonics (rSH) $\mathcal{Y}_{\ell m}$, then

$$u(\mathbf{x}) = \underbrace{\left(\sum_{lm} U_{lm}\mathcal{Y}_{lm}\right)\mathbf{e_r}}_{\text{Radial Component}} + \underbrace{\left(\sum_{lm} V_{lm}\mathcal{Y}_{lm}\right)\mathbf{e_t}}_{\text{Tangential Component}} \quad , \quad \mathbf{l} \geq \mathbf{2}$$

  where the rSH coefficients (U_{lm}, V_{lm}) encode Earth's elastic response and are functions of the load Love numbers $(h_l^{'}, l_l^{'})$.
- JPL-RL06M was expanded in bandlimited $(0 \leq \ell \leq 179)$ rSH coefficients that have then been converted into Stokes, i.e. geopotential, coefficients [10].
- Non-tidal de-aliasing products (ocean and atmosphere) have been restored [4] and the Stokes coefficients were finally detrended.
- Elastic displacements $u(\mathbf{x})$ were computed by using load Love numbers derived from PREM [11]. Note that the $u(\mathbf{x})$ was reconstructed from $\mathcal{Y}_{\ell m}$ within the band $2 \leq \ell \leq 179$, in such a way that they do not reflect the degree-1 surface deformation.

6. Elastic Displacements u(x) from JPL-RL06M (b)

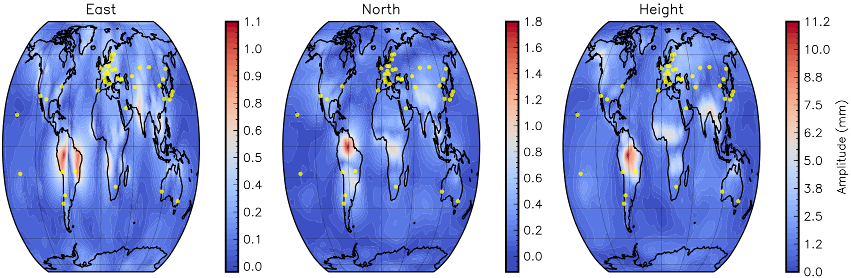

Spatial variability of the annual oscillation of the elastic displacements from JPL Mascon-RL06 determined through the load Love numbers outlined in [11] and based upon PREM [6]. Non-tidal variability of Ocean and Atmosphere has been restored into the Mascons. The elastic displacements deliberately exclude degree-1 and hence do not reflect annual geocenter motion. Yellow dots represent the location of SLR stations.

7. Estimation Model

- At time t_k, with n_s SLR stations simultaneously observing, we can construct the model $\mathbf{Ax} - \mathbf{L} = \mathbf{v}$, solved via least-squares, where
- $\mathbf{L}$ is the vector containing differences of SLR-observed crustal deformation and JPL-RL06 elastic displacements in the local tangent (ENU) space.
- $\mathbf{x} = [\mathbf{c_{10}}, \mathbf{c_{11}}, \mathbf{s_{11}}]$ is the vector of degree-1 surface deformation at t_k
- $\mathbf{A} \in \mathcal{M}_{\mathbf{3n_s \cdot 3}}(\mathbf{R})$ where for the i-th Station:

$$\mathbf{A_i} \quad = \quad \frac{a}{1+k_1^{'}} \cdot \begin{bmatrix} h_1^{'} P_{10}(\mu) & h_1^{'} P_{11}(\mu)\cos(\lambda_i) & h_1^{'} P_{11}(\mu)\sin(\lambda_i) \\ 0 & -\frac{l_1^{'}}{\sin(\theta_i)} P_{11}(\mu)\sin(\lambda_i) & -\frac{l_1^{'}}{\sin(\theta_i)} P_{11}(\mu)\cos(\lambda_i) \\ -l_1^{'}\partial_\theta P_{10}(\mu) & -l_1^{'}\partial_\theta P_{11}(\mu)\cos(\lambda_i) & -l_1^{'}\partial_\theta P_{11}(\mu)\sin(\lambda_i) \end{bmatrix}$$

where $\mu = \cos(\theta_i)$,(θ_i, λ_i) are polar coordinates, a is Earth's radius, $(h_1^{'}, l_1^{'}, k_1^{'})$ degree-1 load Love numbers, P_{lm} the *associated Legendre functions*.

8. Network Shift Approach for SLR-based CM-CN

- First sketched out in the 90's in the context of "fiducial-free" GPS data analysis by Heflin et al. [7], the *Network Shift Approach* entails
  - applying and estimating the parameters of a linearized *similarity transformation* (cf Eqn 2),
  - whose translations (T) are related to (CN-CM) offsets, where CN is the Center-Of-Network.
- The estimation model adopted in this exercize relies upon the following transformation [1]:

$$X_s(t) = X + (t - t_0) \cdot \dot{X} + T(t) + \cancel{\lambda(t)} X + \cancel{\mathbf{R}(t)} X \qquad (2)$$

  Since SLR input SINEX files are rotationally aligned to ITRF prior to the application of Equation 2, R (rotation) parameters are not estimated.

- For a methodological discussion on the *Network Shift* and other approaches to Geocenter Motion determination, the interested reader is invited to consult [see e.g. 5, 8].

9. Comparison of Geocenter Motion (CM-CN) Time Series

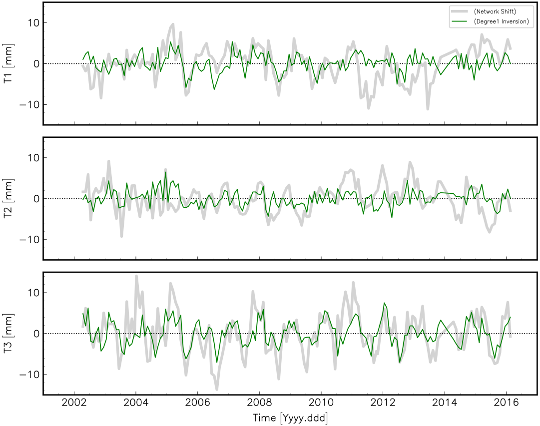

Time series of (CM-CN) as determined through the Network Shift approach (gray thick line) and the Degree-1 Spectral Inversion (green line). Both the time series result from equally weighted observations, i.e. the measurement covariance matrix is assumed to be the identity **I**.

10. Comparison of Seasonal Geocenter Motion (CM-CN)

Approach		Annual		Semi-Annual	
		A [mm]	φ [deg]	A [mm]	φ [deg]
Degree1	T_x	1.2 (0.2)	342.7 (8.7)	0.3 (0.2)	173.1 (3.8)
	T_y	0.8 (0.2)	296.9 (7.9)	0.3 (0.2)	120.1 (5.1)
	T_z	2.8 (0.2)	307.9 (4.4)	0.4 (0.2)	162.5 (4.7)
Net Shift	T_x	2.4 (0.4)	319.1 (9.0)	0.4 (0.4)	189.2 (7.6)
	T_y	2.9 (0.3)	244.9 (5.2)	0.6 (0.3)	201.7 (6.6)
	T_z	4.2 (0.5)	297.4 (6.0)	1.0 (0.5)	119.2 (11.4)

The model adopted for the least squares fit of the seasonal terms is $A \cdot \sin\left[\omega(t - t_0) - \varphi\right]$, where $\omega = 2\pi/\tau$, with $\tau = 1, 0.5$ yr, and t_0 January 1 2005. Amplitudes A are given in *mm*. Phases φ are in *deg*. Parenthesized are $1 \cdot \sigma$ formal errors.

Acknowledgments

- This work was carried out at the Jet Propulsion Laboratory, California Institute of Technology, under a contract with the National Aeronautics and Space Administration (NASA).
- We gratefully acknowledge funding support from NASA's Space Geodesy Program and from NASA ROSES (GRACE) Program NNH15ZDA001N-GRACE.
- Cinzia Luceri (e-geos) and Antonio Basoni (e-geos) are gratefully acknowledged for providing the ASI-SLR preliminary solution.

References

[1] Altamimi, Z., Sillard, P., and Boucher, C. (2007). CATREF software: combination and analysis of terrestrial reference frames. Technical report, Laboratoire de Recherche en Godsie, IGN, Paris, Tech Rep.

[2] Appleby, G., Rodríguez, J., and Altamimi, Z. (2016). Assessment of the accuracy of global geodetic satellite laser ranging observations and estimated impact on ITRF scale: estimation of systematic errors in LAGEOS observations 1993-2014. J Geodesy, **90**(12), 1371–1388.

[3] Chanard, K., Fleitout, L., Calais, E., Rebischung, P., and Avouac, J. P. (2018). Toward a Global Horizontal and Vertical Elastic Load Deformation Model Derived from GRACE and GNSS Station Position Time Series. J Geophys Res-Sol Ea, **123**(4), 3225–3237.

[4] Dobslaw, H. and Dill, R. (2018). Predicting Earth orientation changes from global forecasts of atmosphere-hydrosphere dynamics. Adv Space Res, **61**(4), 1047–1054.

[5] Dong, D., Yunck, T., and Heflin, M. (2003). Origin of the International Terrestrial Reference Frame. J Geophys Res Sol-Ea, **108**(B4).

[6] Dziewonski, A. M. and Anderson, D. L. (1981). Preliminary reference Earth model. Phys Earth Planet Inter, **25**(4), 297 – 356.

[7] Heflin, M., Bertiger, W., Blewitt, G., Freedman, A., Hurst, K., Lichten, S., Lindqwister, U., Vigue, Y., Webb, F., Yunck, T., and Zumberge, J. (1992). Global geodesy using gps without fiducial sites. Geophys Res Let, **19**(2), 131–134.

[8] Lavallée, D. A., van Dam, T., Blewitt, G., and Clarke, P. J. (2006). Geocenter motions from GPS: A unified observation model. J Geophys Res-Sol Ea, **111**(B5). B05405.

[9] Mitrovica, J. X., Davis, J. L., and Shapiro, I. I. (1994). A spectral formalism for computing three-dimensional deformations due to surface loads: 1. Theory. J Geophys Res-Sol Ea, **99**(B4), 7057–7073.

[10] Wahr, J., Molenaar, M., and Bryan, F. (1998). Time variability of the Earth's gravity field: Hydrological and oceanic effects and their possible detection using GRACE. J Geophys Res-Sol Ea, **103**(B12), 30205–30229.

[11] Wang, H., Xiang, L., Jia, L., Jiang, L., Wang, Z., Hu, B., and Gao, P. (2012). Load Love numbers and Green's functions for elastic Earth models PREM, iasp91, ak135, and modified models with refined crustal structure from Crust 2.0. Comput and Geosci, **49**, 190 – 199.

[12] Watkins, M. M., Wiese, D. N., Yuan, D.-N., Boening, C., and Landerer, F. W. (2015). Improved methods for observing Earth's time variable mass distribution with GRACE using spherical cap mascons. J Geophys Res Sol-Ea, **120**(4), 2648–2671.